Journal Name

Dynamic Article Links ►

Cite this: DOI: 10.1039/c0xx00000x

www.rsc.org/xxxxxx

ARTICLE TYPE

BRET-linked ATP assay with luciferase

Golnaz Borghei and Elizabeth A H Hall*

Received (in XXX, XXX) Xth XXXXXXXXX 20XX, Accepted Xth XXXXXXXXX 20XX
DOI: 10.1039/b000000x

Taking advantage of BRET, a mutant firefly luciferase with higher pH- and thermo-stability than the wild-type could be coupled with the red-emitting fluorescent protein of mCherry in both a fused and unfused format. The BRET pair allows >40% of the light emitted to be red shifted over 600nm to the mCherry acceptor wavelength. Taking the expected quantum yield for mCherry (0.22), a good fit to predicted light transfer is shown, with no other losses. Two measurements are considered for ATP determination: a) a ratiometric technique for ATP measurement using both donor and acceptor emission intensities, making the calibration slope independent of protein concentration in a broad range. This measurement was limited by the BRET efficiency and the low quantum yield of the mCherry acceptor, but this detection limit might be improved with other fluorescent proteins with higher quantum yield. The fused BRET pair also resulted in a small increase in the BRET ratio. b) an ATP dependent shift in the wavelength maximum using just the acceptor mCherry emission was also proposed for ATP determination. This did not require a high BRET efficieny and only uses emisson above 600nm to obtain the acceptor emission maximum, but not its intensity; it is independent of protein concentration across a broad range. This offers a novel and robust method for determination of ATP between 10^{-11} - 10^{-5} M with an easy baseline calibration with ATP concentration >10^{-4} M.

Introduction

ATP, as the universal energy source for cellular function, is present in every type of biological cell and plays a critical role in energy exchange[1]. Therefore ATP measurement is crucial in analysis of cellular mechanisms, enzymatic processes and biosynthesis[2]. Furthermore, since all living organisms contain ATP, it finds widespread application in diagnostic assays of toxicity and contamination by microorganisms in varied fields such as the pharmaceutical industry, blood banks, food and water processing and environmental pollution[3].

Among the simplest methods for ATP measurement are chromogenic and colorimetric techniques in which a result can often be read by eye[1,4,5]. However, probably the most promising and most studied approach to ATP measurement has been enzyme-linked. Since ATP is critical in numerous enzyme pathways, there are many possibilities to exploit assays designed for a selective enzyme substrate, formatted so they are limited by the ATP concentration, rather than the primary substrate concentration. In this context, due to its high sensitivity and selectivity, the bioluminescent firefly luciferase (Fluc) -based assay still remains the most widely used technique to measure ATP[6]. The firefly luciferase enzyme reaction has a fast response (milliseconds) and a broad range for ATP detection. Other adenosine-containing nucleotides such as AMP or adenosine diphosphate (ADP) do not react with the enzyme, so the reaction is highly specific to ATP. Theoretically sensitivity is extremely high, because there should be no background signal in the absence of ATP[2]. Nevertheless, ATP measured down to the attomole level still requires low noise instrumentation[7,8] to resolve the signal[2] with any background signal due to extraneous light eliminated[9].

Another problem encountered in complex media and tissues which absorb a large proportion of the light below 600 nm, is the short wavelength of emission for the luciferase-luciferin (Fluc-LH_2) system (~550 nm). Attempts to shift the emission wavelength through derivatisation of luciferin have been successful in terms of wavelength shift (eg the 6' amino derivatives have produced red-shifts up to to 625 nm)[10] but at the cost of light output, thus other ways to circumvent these limitations could be beneficial for some ATP assays.

Bioluminescence Resonance Energy transfer (BRET) is a natural phenomenon occurring in marine organisms such as *Aequorea* jellyfish and the sea pansy Renilla reniformis. It is a technique that has also been applied for noninvasive monitoring of BRET in live cells and whole-animal imaging[11-13]. Since the development of the first engineered BRET probe in 1998[14], it has been widely used in analytical biosensing and imaging particularly via conjugation of luciferase enzymes as donors and fluorescent proteins as acceptors[15-18]. Despite red-emitting fluorescent proteins (RFPs) having the advantage of long wavelength emission, use of red-emitting fluorescent proteins as acceptors in the general development of BRET systems is not as advanced and diverse as the use of GFP variants. The main reasons are that fewer monomeric RFP variants were available, as well as the lower quantum yield and brightness of these

fluorescent proteins.

The most common application of BRET pairs introduced thus far has been in detection of protein-protein interactions (PPIs)[11,13,15,19,20]. Arai et al introduced the first red-emitting BRET system employed in a PPI, shortly after the discovery of RFPs. This used firefly luciferase as the donor and tetramer DsRFP as the acceptor[21] (Quantum yield of DsRFP is 0.79). Among other successful luciferase-fluorescent protein fusion combinations that have been reported are Rluc-GFP [22], Rluc-mOrange[23], Fluc-mKate[24], Fluc-mCherry[25] and Rluc-EYFP[13,26]. Despite the reasonable performance of these BRET systems, most effort has been focused on their functionality as both an autofluorescent protein and a fluorescently tagged bioluminescent probe for *in vivo* imaging[12,17,22, 23, 26]. Noninvasive assesment PPIs in cell cultures or tissues has always been of special interest due to their core role in understanding diseases and providing theraputic targets.

In analytical biosensing and imaging, bioluminescence and BRET have distinct advantages over fluorescence and Föster Resonance Energy Transfer (FRET). BRET does not require excitation of the donor by light, therefore shows significant lower background signal compared to FRET. Furthermore, the probability of undesirable direct excitation of the acceptor or photobleaching of the fluorophores, which are common drawbacks in FRET, are insignificant in BRET. In tissue imaging applications, BRET is thus more applicable than FRET for photoresponsive cells (e.g. retina cells and most plant tissues) or autofluorescent tissues (containing molecules such as NADH, collagen or flavins). Direct excitation in FRET can damage the tissue induced by a photogenerated chemical agent and adverse photochemical reactions. In addition, light sensitive pigments in photoresponsive tissues can react with specific wavelengths of light resulting in the activation of photosensitive biological processes.

Therefore, in a number of reports, BRET-based assays have been extended to study PPIs in living cells[11,12,27,28]. For example, Dragulescu-Andrasi et al have used BRET-based red-light emitting reporters to ratiometrically measured protein-protein interactions in deep-tissue small animal tumour models[29]. In another work, "BRET3", a BRET-based probe composed of mOrange fluorescent protein (λ_{Em} 560 nm[30]) and a mutant Renilla *luciferase* (RLuc8) employs red emission to observe biological signals from live single cells as well as from superficial and deep-tissue structures[31]. Recently a fusion protein of an enhanced YFP variant, Venus, and the RLuc8 was developed, which offers a BRET-based ratiometric Ca^{2+} indicator[26]. However, this luciferase enzyme does not use ATP as cofactor.

On the other hand, fusion proteins of firefly luciferase with fluorescent proteins (Fluc-FP) do offer a dual colour protein with the potential for developing a useful ratiometric ATP measurement from the bioluminescence properties of luciferase and the fluorescence properties of fluorescent proteins. Such a dual signal measurement may be able to overcome issues of variability in signal intensity causing erroneous results. In another work, Branchini et al designed a sequential BRET-FRET system employing a firefly luciferase, red-emitting mKate fluorescent protein and nIR fluorescent dyes[24]. In this instance the ratiometric luminescent probe was used to assay protease activities.

Here we examine a BRET-based technique for ATP measurement. A mutant firefly luciferase (x5) with higher pH- and thermostability than the wild-type luciferase (Fluc)[32] was selected, coupled with mCherry[30] as a BRET-based probe for ATP measurement. The combination of x5 Fluc with mCherry shifts some of the luminescent emission wavelength to the red, so that together with the greater pH- and thermostability for the x5 firefly luciferase mutant, this could offer potential benefits either in the fusion protein format or the unfused protein, for BRET-based ATP measurement techniques.

Materials and Methods

D-luciferin, ATP and EDTA, were purchased from Sigma-Aldrich UK. Taq DNA polymerase and KOD Hot Start DNA Polymerase used for polymerase chain reaction (PCR), were purchased from Novagen. QuikChange II XL Site-Directed Mutagenesis Kit was purchased from Agilent Technologies and applied as per manufacturer's protocol. Enzymes used for cloning (restriction enzymes, calf intestinal alkaline phosphatase, Antarctic phosphatase, T4 DNA ligase) and Quick Ligation kit were purchased from New England Biolabs and were used according to the manufacturer's instructions. Plasmid pET16b (Novagen) containing x5 luciferase gene was a gift from Dr Erica Law, University of Cambridge. Plasmid pRSET B, containing the mCherry sequence, was kindly provided by Dr Allison Denis from Prof Gang Bao's team at Georgia Tech University. *Epicurian Coli*® XL10-Gold ultracompetent cells were purchased from Stratagene and transformation was carried out as per manufacturer's protocol.

Construction of mCherry-Fluc fusion protein

The pRSET B vector encoding x5-luc was used as a template for mCherry-Fluc fusion protein construction. The vector was subjected to site directed mutagenesis aimed to add two restriction sites of NdeI and BamHI for later insertion of the Fluc gene, while the stop codon was placed at the end of the sequence. The linker between mCherry and Fluc in the fusion protein consisted of the original seven aminoacid tail of mCherry, inserted by Shaner et al[30] (plus one extra aminoacid of His), giving a linker sequence of: Gly, Met, Asp, Glu, Leu, Tyr, Lys, His. The resultant sequence was confirmed using the DNA Sequencing Facility, Department of Biochemistry, University of Cambridge.

Expression and purification of His-tagged proteins

Before expressing the protein, BL21(DE3) E. coli containing the desired plasmid were grown overnight in a starter culture of 15 ml Luria Broth (LB). The culture was then transferred into 200 ml fresh LB medium; grown to mid-log growth phase (OD600 = 0.4 to 0.6) and induced with isopropyl β-D-thiogalactoside (IPTG). For expression of mCherry and x5-luc 1 mM IPTG were added at 25°C for 8 hrs. The fusion protein of mCherry-Fluc (CL) was expressed at 25°C with 0.1 mM IPTG resulting in the pure fusion protein of CL. Purity of proteins was analysed using SDS/PAGE (results not shown).

Induced cells were collected by centrifugation (RC-5C centrifuge, Sorvall) at 9,500 rpm and 4°C for 10 min using the F10-6x500y rotor. The cell pellet was frozen and kept at -80ºC overnight. All processes of cell lysis and protein purification were carried out at 4°C. Cell pellets were resuspended with 5 ml/g wet cells in the lysis buffer (10 mM phosphate buffer, pH 8.0, 2.7 mM KCl, 0.3 M NaCl, 10 mM 2-mercaptoethanol, 20 % (v/v) glycerol, 1×

EDTA- free protease cocktail inhibitor with 2 % (v/v) Triton X-100 and 20 mM imidazole) following by addition of 124 units/g wet cells benzonase® nuclease. Thawed resuspensions were mechanically pressed and put through three freeze – thaw cycles. All proteins were purified with the same technique previously described by Law et al[32] using Ni-NTA agarose beads followed by PD-10 desalting columns. Protein concentrations were estimated with the Bradford method[33] using the Coomassie Blue protein assay reagent kit from Pierce as per manufacturer's protocol, with BSA as the standard.

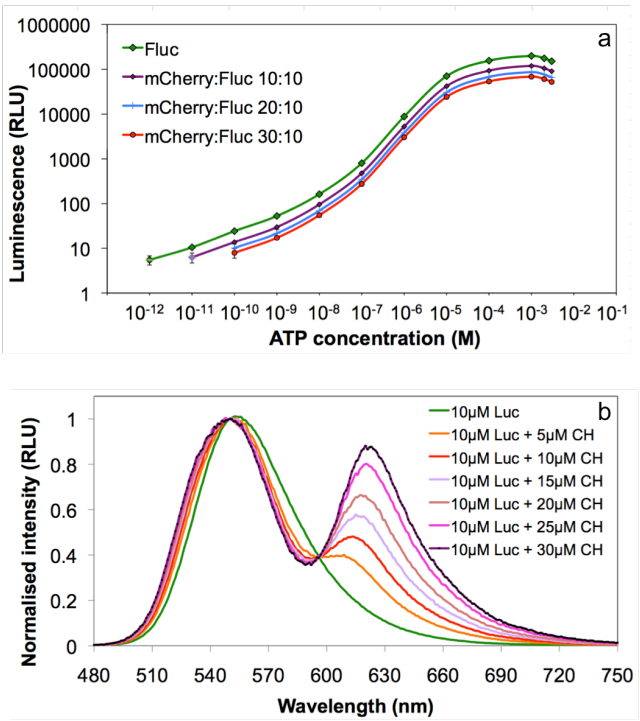

Fig.1 ATP measurement with BRET-based probes compared to x5 firefly luciferase. Luciferin concentration was 200 μM. Fluc concentration was fixed at 10 μM in all probes whilst the mCherry concentration was varied. (a) The concentrations used were: 10 μM x5 firefly luciferase, 10, 20 and 30μM mCherry. The y-axis shows the total emission output at 30 ± 5 seconds after ATP solution injection. Data were collected with a luminometer and correspond to relative total emission >270 nm. Bioluminescence measurements were carried out independently three times. (b) Constant concentration of Fluc (Luc) at 10 μM, with increasing concentration of mCherry (CH) from 5 to 30 μM. The spectra is normalised at the first peak around 550 nm. The graph shows the increase in BRET ratio with the increase in the acceptor (mCherry) concentration.

ATP measurement

Two probes were used to measure ATP based on BRET: (a) unfused mCherry and x5 Fluc in different concentration ratios of 5:10, 10:10, 20:10 and 30:10 mCherry:Fluc (Fluc concentration was fixed at 10 μM), (b) pure mCherry-Fluc (CL) fusion protein expressed at 25°C. All probes were made in TEM buffer (0.1 M Tris/acetate, pH 7.8, 10 mM $MgSO_4$ and 2 mM EDTA) containing 200 μM D-luciferin (D-LH_2). A range of fresh ATP solutions (picomolar to millimolar concentrations) was prepared in UHP water. The data were read with both luminometer (Labsystems Luminoskan Ascent luminometer with Ascent software) which collects all emission above 270 nm and fluorometer (Cary-Eclipse fluorescence spectrophotometer (Varian)). The data were collected at 30 ± 5 seconds after the manual injection of ATP solution.

BRET ratio calculation

BRET ratio was measured with the fluorometer; the data were read at two peak-maxima wavelengths of typically 550 ± 5 nm and 615 ± 5 nm. The BRET ratio calculations were obtained by dividing the emission intensity at the secondary (mCherry) peak maximum (615 ± 5 nm) by emission intensity at the first (excited state of LH_2 oxidation product) peak maximum (550 ± 5 nm).

Results and Discussion

ATP linked emission with BRET pairs

Unfused mCherry and Fluc

Figure 1a compares the luminescent intensity (all emission >270nm) for unfused BRET-probes of mCherry and Fluc in the presence of ATP and luciferin, for a constant concentration of Fluc; this shows a small decrease in overall light output with increase in mCherry concentration. This is connected with an emission profile that has shifted to longer wavelengths, consistent with resonant energy transfer to mCherry (fig. 1b), so that this reduction could be linked with the quantum yield for the fluorescent protein being <1 (QY for mCherry = 0.22[30]). For example, in this comparison, Fluc has a limit of detection of ~1 pM ATP, but the lower total emission output with increase in resonance energy transfer to the fluorescent protein raises the detection limit so that for 30:10 μM mCherry:Fluc the limit has increased to 0.1 nM.

To explore whether the losses can be attributed entirely to the QY of the flurorescent protein (FP), the mCherry emission output can be predicted by considering the reduction in the fluorescence at the FP emission, due to the quantum yield of the fluorescent protein (QY_{FP}), from the intensity of Fluc emission in the presence of FP (B) and the absence of FP (B_0) at the same concentration, according to:

$$I_{tot} = B_0 - \left(1 - \frac{B}{B_0}\right)B_0 + \left(1 - \frac{B}{B_0}\right)B_0 QY_{FP} \qquad \text{.....(1)}$$

which allows the intensity of the fluorescent protein emission to be estimated according to:

$$I_{FP} = \left(1 - \frac{B}{B_0}\right)B_0 QY_{FP} \qquad \text{.....(2)}$$

Assuming a QY for mCherry of 0.22, Figure 2 demonstrates a remarkable fit between predicted and experimental data for the mCherry+Fluc combination (increasing mCherry Figure 2A). This also applies when the overall protein concentration is changed for a given mCherry:Fluc ratio (Figure 2B for 1:1 ratio), indicating that there are no 'dark quenching' reactions between the fluorescent protein and Fluc, reducing the total light output. This infers that the total luminescence and the BRET ratio (I_{FP}/I_{Fluc}) are predictable, knowing the concentration and quantum yield of the acceptor, once the Stern-Volmer (K_{SVBL}) constant for the BRET pair is known (figure 3C):

$$\left(1 - \frac{B}{B_0}\right) = \frac{1}{K_{SVBL}} \qquad \text{.....(3).}$$

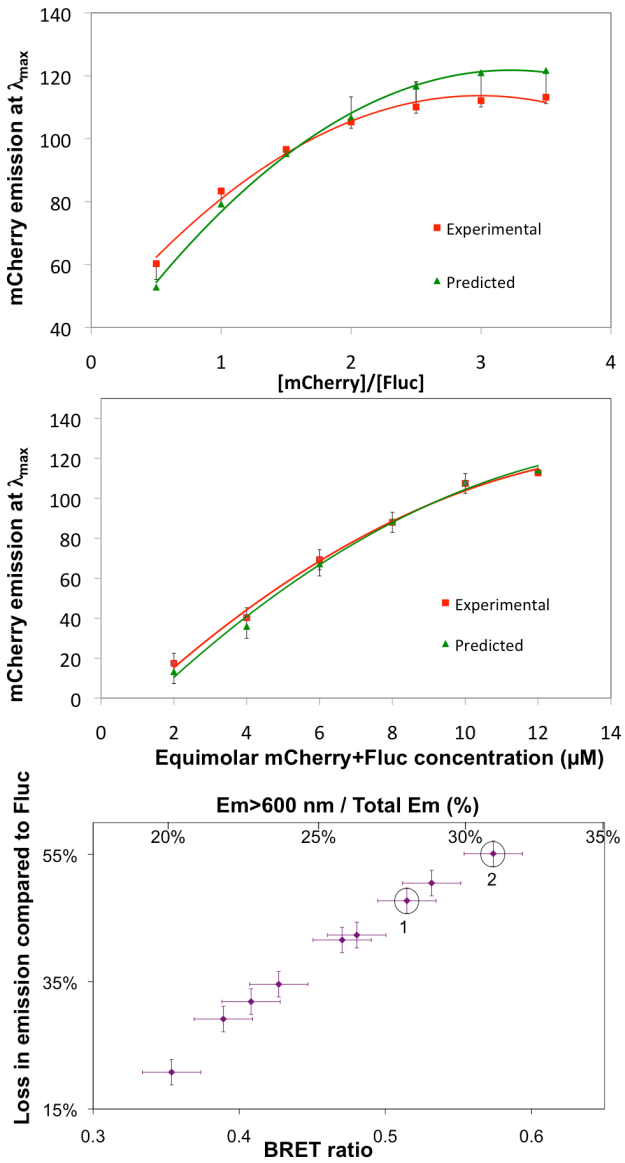

Fig.2 Predicted intensity at secondary peak (corresponding to mCherry emission) verses the experimental data. (a) constant concentration of Fluc at 10 μM, with increasing concentration of mCherry. (b) equimolar mCherry+Fluc from 2 to 12 μM, . This suggests that the fluorescence emission is accurately predictable Shows no hidden loss of energy during the BRET mechanism. (c) Relation between loss in total emission (compared to equimolar Fluc), BRET ratio and percentage shift to above 600 nm in 1:1 combination of mCherry:Fluc (fusion protein and equimolar unfused proteins). By measuring the BRET ratio, the loss in total emission and the light shift can be predicted (see text). Black circles on the graph represent the maximum BRET ratio obtainable by: (1) equimolar mCherry+Fluc (2) CL fusion protein.

ATP measurement via the BRET ratio

It follows from the discussion above that trying to increase resonance energy transfer is thwarted by losses due to the QY of the fluorescent protein. Thus, a lower [FP] yields a higher light output and from the previous derivations, the ratio between the emission intensity due to donor and acceptor in the BRET pair is a function of ATP concentration, as can be seen visually in Figure 3a. Thus, while the decrease in ATP concentration results in a decrease in the overall emission from the donor (Fluc-substrate complex) the BRET ratio increases (Fig. 3b) and the BRET ratio is a function of [acceptor]/[donor]. Depending on the acceptor concentration, lower detection is still limited by the QY for the acceptor. With this configuration, the BRET ratiometric measurement of ATP could be resolved down to 10-100 pM. Furthermore, for 10:10 - 10:25 mixtures, the slope of the BRET ratio calibration curve below 10^{-8}M is independent of protein concentration, which makes it a robust method for ATP measurement.

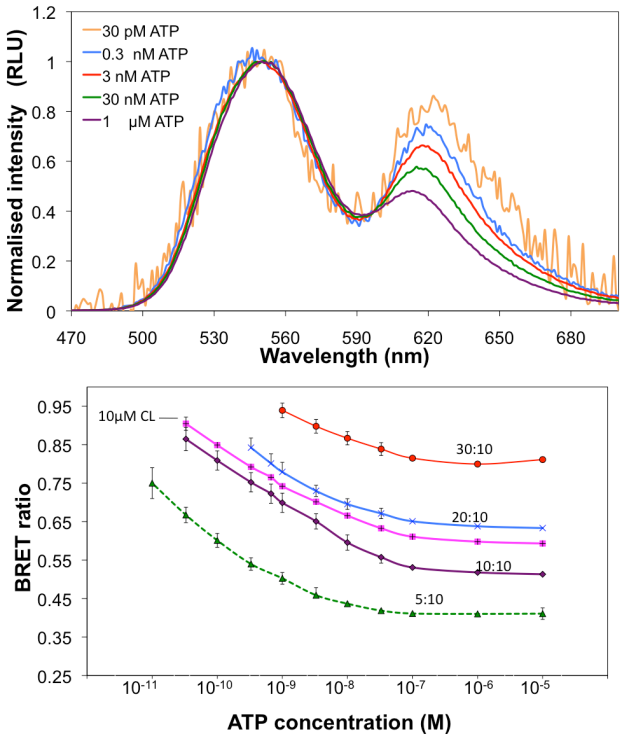

Fig. 3. (a) A BRET probe consisting 10:10 μM [mCherry]:[Fluc] unfused proteins. Normalised intensity at the BRET emission wavelengths with ATP concentration . (b) The change in BRET ratios as a function of ATP concentration for unfused BRET pairs with different ratios of [mCherry]:[Fluc] with constant Fluc concentration at 10 μM and mCherry concentration from 5 to 30 μM. This is compared with the fused probe (CL) at 10 μM mCherry-Fluc fusion protein. The trend is constant in different probes and the data is independent of sensitivity (PMT) of fluorometer.

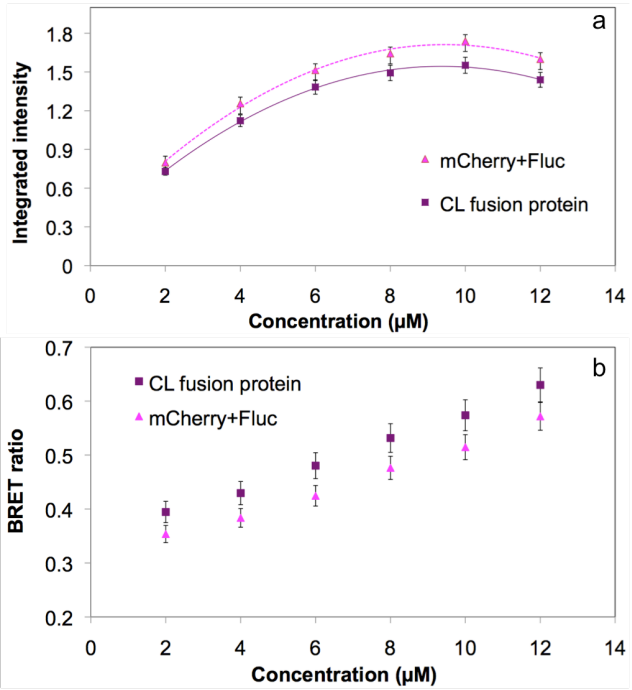

Fig.4 a) Relative integrated intensity and (b) BRET ratio of equimolar concentrations of CL fusion protein (10 μM), in comparison with unfused equimolar of mCherry+Fluc (10:10 μM) are shown. 5% variations between experiments (n=4). Data were collected with fluorometer. All proteins were expressed and purified under the same conditions as the fusion proteins (25°C, 8 hrs, 0.1 mM IPTG). Proteins were prepared in TEM buffer. The substrate consists of 200 μM D-luciferin, 1 mM ATP and 10 mM $MgSO_4$. Data were at 30 ± 5 seconds after substrate injection.

Fused mCherry-Fluc (CL)

Based on this, it can be seen in Fig. 3b that a Fluc-mCherry fusion protein (CL) (with a forced intramolecular 1:1 ratio) follows a similar trend to the 10:10 mCherry:Fluc as would be expected, but the ratios are distinct from the unfused counterpart. A comparsion between the total emission (Fig. 4a) and the BRET ratio (Fig. 4b) of a fusion protein of mCherry-Fluc (CL) and equimolar mCherry+Fluc confirms this and reveals the probable contribution of inter- and intra-BRET in the FP-Fluc pair. Referring back to figure 2 (points 1 and 2) shows that the intensity of the emission above 600nm can still be predicted according to equation 2, depending on the QY of the acceptor. However, as seen in Fig. 4a, a CL fusion protein with a controlled 1:1 ratio produces ~10% lower luminescence emission compared with the unfused proteins (Fig. 3b, 4b), but maintains the slope of the calibration curve as for the unfused proteins. To confirm this difference, a paired t-test was used (two-tailed, df=5). CL fusion protein compared to unfused proteins shows p-value of $1.2x10^{-5}$ with mean of the difference=$5.3x10^{-2}$, suggesting a significant difference between the BRET ratios with calculated p-values below 0.05 (95% confidence interval). This does not show whether this is just due to a change in the geometric terms in the Förster equation as a result of the fusion, in particular r^6 describing the inter-fluorophore distance or κ, describing the dipole orientation, or some other change in Fluc kinetics. However, it does establish some vulnerability in an intensity based measurement for ATP.

ATP measurement as a function of acceptor wavelength maximum

It can be seen that at 10:10 μM Fluc:mCherry, ~28% of the light has been shifted above 600nm (Table 1), whereas a CL fusion protein achieves ~32% and 10:25μM Fluc:mCherry ~40% above 600nm. This transfer of light above 600nm is a significant advantage. However, for measurements in tissues, with background autofluorescence below 600nm, the BRET ratio may still be compromised by needing the measurement of luciferase emission below 600nm against this background for the ratiometic measurement. However, for ATP concentrations above 10^{-11} M, there is a well resolved wavelenth maximum for the BRET emission above 600nm for all Fluc:mCherry or CL. This leads to another novel approach to a BRET measurement.

Concentration (μM)	Limit of ATP detection (M) by BRET ratio	Relative light output (%)	Photons above 600 nm / total (%)
10 Fluc	10^{-12} - 10^{-13}	100	13
10:5 μM Fluc:mCherry	10^{-11} - 10^{-12}	75±5	22±2
10:10 μM Fluc:mCherry	10^{-10} - 10^{-11}	55±5	28±2
10:20 μM Fluc:mCherry	10^{-9} - 10^{-10}	45±5	37±2
10:30 μM Fluc:mCherry	10^{-9} - 10^{-10}	34±5	44±2
10 μM CL	10^{-10} - 10^{-11}	50±5	32±2

Table 1 Comparison of light emitted above 600nm for different Fluc:mCherry combinations and CL fusion protein, normalised to totallight output by Fluc at the same concentration of 10μM.

The idea that the fusion protein geometry highlights the energy transfer due to dipole or distance, leads to examination of the mechanism of the bioluminescence. Excitation to the oxyluciferin* state causes an increase in the dipole moment and reverses its direction[34,35] leading to disruption of bonds between oxyluciferin* and the enzyme binding site with partial dissociation of the enzyme-oxyluciferin* complex. Emission and deactivation can occur from either the associated or dissociated oxyluciferin*[36,37]. The kinetics of this reorganisation causes conformational changes in the oxyluciferin* (including keto-enol tautomerism, scheme 1), which may result in a green or red shift in the fluorescent emission, imposed by interaction with the active site, which determines the final emission wavelength and peak broadening for a particular luciferase.

Cite this: DOI: 10.1039/c0xx00000x

www.rsc.org/xxxxxx

ARTICLE TYPE

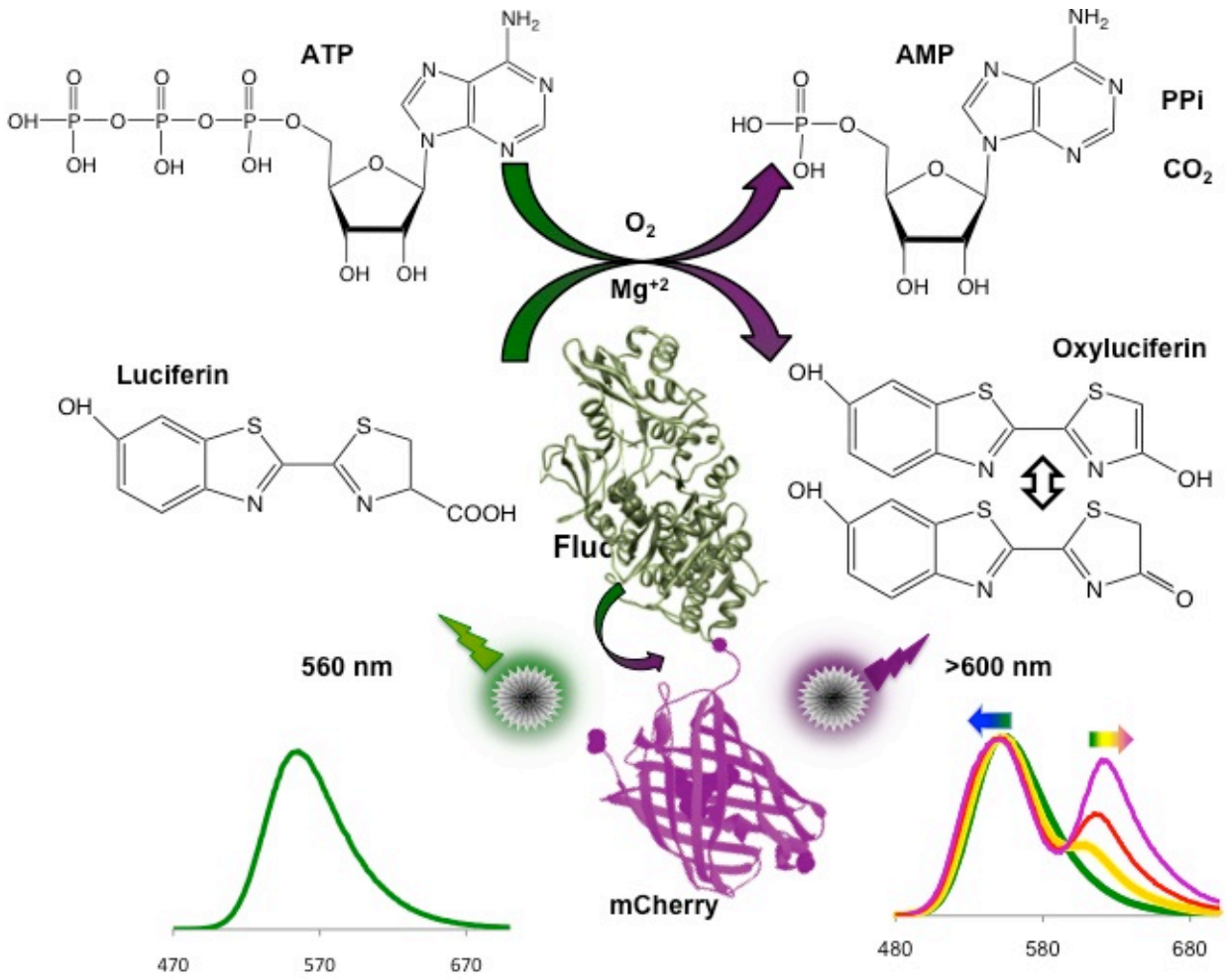

Scheme 1 BRET in Luciferase-Luciferin reaction: Luciferase acts as enzyme and donor, while mCherry is the acceptor. ATP measurement via the luciferase-luciferin signal (on the left) and the BRET pair signal due to the luciferase-luciferin donor and mCherry acceptor (on the right). Conformational changes in the oxyluciferin* (including keto-enol tautomerism), results in a green or red shift in the fluorescent emission

Rebartz et al[38] has disentangled the keto–enol tautomerism for oxyluciferin to identify the individual spectral contributors. This works suggests that the spectra range from the phenol-enol at low wavelengths through phenol-keto < phenolate-enol < phenolenolate < phenolate-enolate to phenolate-keto at highest wavelength. These equilibria are dependent on protonation, which in luciferase is served through the amino acid interactions in the active site. Since luciferase-bound luciferyl adenylate is one of the first intermediates in the mechanistic pathway, it might be postulated that at low ATP concentration, the conformational reorganization which results in changes in this equilibrium would result in an ATP dependent product, and that the tautomer and its level of protonation could be revealed through measurement of the absorption spectra and possibly also the emission wavelength of the excited state oxyluciferin product.

The small blue shift in donor (Fluc) wavelength seen here, with increase in ATP concentration is consistent with such a change in the keto-enol ratio due to the reorganisation of the oxyluciferin*, influenced by the concentration of ATP. However, the shift is small and not adequate to be correlated directly with [ATP].

On the other hand, the increase in ATP concentration is also accompanied by a red-shift in the acceptor peak corresponding to mCherry fluorescence emission (Figure 5a). This is a much larger shift, which can be correlated to [ATP]. mCherry has an emission

maximum of 611-613nm when excited at 587nm[39], but as can be seen in figure 5b, the mCherry emission spectrum is dependent on excitation wavelength. At 10µM mCherry has a maximum emission <614nm when excited around 580nm (figure 5b), but reached a maximum 621±1nm when excited in UV Range (<300 nm). So, we can correlate the shift in acceptor emission wavelength to a shift in excitation (donor) wavelength due to an ATP-dependent change in the oxyluciferin* reorganisation.

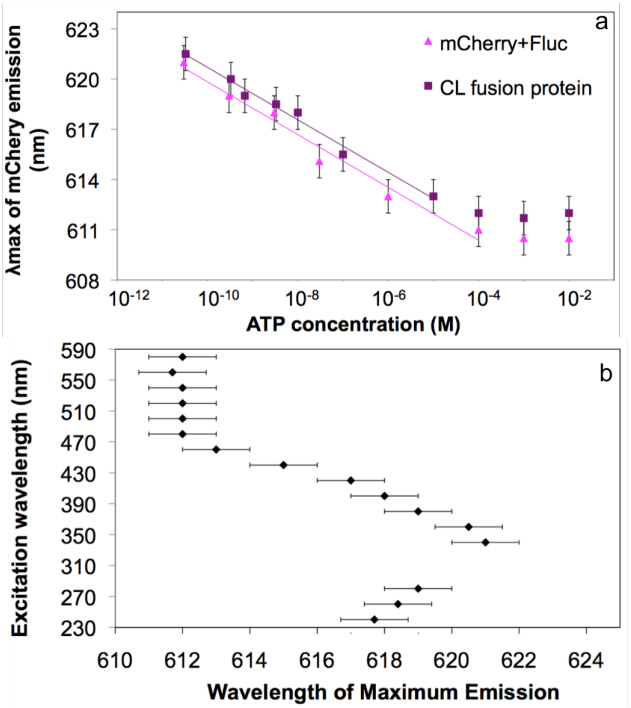

Fig.5 (a) The change in the wavelength of mCherry fluorescence maximum emission in a BRET pair of 10:10 µM [mCherry]:[Fluc] and CL fusion protein. The graph shows a blue-shift in the maximum emission wavelength with an in increase in ATP concentration (donor emission) with constant acceptor concentration (Error: ±1 nm). (b) mCherry (10 µM) excited at different wavelengths. mCherry emission excited at UV range appears at longer wavelengths than excitation in visible range.

This leads to a robust ATP dependent calibration: like the BRET ratio measurement, the slope of the calibration curve for mCherry λ_{max} vs ATP is independent of fused or unfused protein in the range 10^{-11} - 10^{-5}M ATP and has a 'baseline' calibration independent of concentration above 10^{-4}M (figure 5a). This produces a calibration of:

$$\lambda_{obs} - \lambda_{[ATP]>10^{-4}M} = x$$
$$[ATP]=10^{-(4+0.74x)}\ \mathrm{M}$$

Importantly, this is the first ATP dependent measurement of BRET that can be performed exclusively above 600nm.

Conclusion

A BRET-based measurement of ATP suggests some potential advantages over a conventional method employing pure Fluc. Emission above 600nm becomes possible rather than the conventional pure firefly luciferase in which the emitted green light is largely absorbed by the tissue. By employing fused or unfused mCherry and Fluc, the BRET structure can transfer more than 45% of the output light to wavelengths above 600 nm dependent on [ATP]. However, on the down side, since the quantum yield for mCherry is only 0.22[30], the BRET mechanism results in a significant overall intensity loss. Improved BRET efficiency with recently reported red-emitting fluorescent proteins such as mKate2[40] could be a good alternative due to its high brightness (0.4 compared to 0.22 of mCherry), or eqFP650 can be used for a more red-shifted emission (Em max at 635 nm)[41], so that the BRET method does have a greater potential than achieved with this BRET pair.

Additionally, ratiometric measurement of the BRET donor and acceptor, as proposed here, provides a method that is independent of protein concentration within a broad range and resiliant to any protein loss with time. There is a higher energy transfer for the fusion protein of CL, probably associated with transfer distance and dipole orientation and is attractive for in vivo measurement of ATP, where position of the members of a BRET pair may be difficult to manage otherwise.

Despite the advantages, a main drawback is the ongoing need to obtain a measurement at the lower Fluc wavelength as well as the longer wavelength FP, so that a novel alternative approach that avoids intensity measurements, relating ATP concentration to the red shift in the mCherry emission wavelength, provides an interesting alternative for ATP measurement. We propose that the BRET pair allows fast energy transfer from an unstable high energy green shifted conformer of the ATP-oxyluciferin*-enzyme complex, before its rearrangement. The result is that the BRET is dominated by this transfer at low [ATP] (below K_M), but at higher concentrations RET originates from the Fluc emission >540nm. Since excitation wavelength dependent emission is also a feature seen in other FPs, there is potential for transfer to other FPs and better λ_{max} resolution at lower concentrations with the brighter FPs like mKate2.

Notes and references

Address, Institute of Biotechnology, Department of Chemical Engineering and Biotechnology, University of Cambridge, Tennis Court Road, Cambridge, CB2 1QT.; Tel: 44 1223 334149; E-mail: lisa.hall@biotech.cam.ac.uk

1 P. Mahato, A. Ghosh, S. K. Mishra, A. Shrivastav, S. Mishra, A. Das. *Inorganic Chemistry*, 2011 **50 (9)**, 4162-4170.
2 Z.Wang, P. G. Haydon, E. S. Yeung, *Anal Chem* 2000, **72,** 2001–2007.
3 G. Borghei, E. A. H Hall ATP Measurement in Bio-Contamination. NATO Science for Peace and Security Series A: Chemistry and Biology, ed. Nikolelis, D. P. Springer, 2012, 213-226.
4 A. Buryak, F. Zaubitzer, A. Pozdnoukhov, K. Severin, *J Am Chem Soc* 2008, **130**, 11260–11261.
5 F. Sancenón, A. Descalzo, R. Martínez Máñez, M. Miranda, J. Soto, *A Angew Chem Int Edit* 2001, **40**, 2640–2643
6 P. Costa, N. Andrade, F. Passos, S. Brandão, C. Rodrigues, *Brazilian Archives of Biology and Technology* 2004, **47**, 399–405.
7 B. R. Branchini, D. M. Ablamsky, A. L. Davis, T. L. Southworth, B. Butler, F. Fan, A. P. Jathoul, M. A. Pule, *Anal Biochem* 2010, **396**, 290–297.
8 B. Rice, M. Cable, M. Nelson, J Biomed Opt 2001, 6, 432–440.
9 L. Ceresa, P Ball, *Encyclopedia of rapid microbiological methods* 2006, **2**, 233-250.
10 G R Reddy, W C. Thompson, S. C. Miller. *J. Amer. Chem.Soc.* 2010, **132(39),** 13586-13587
11 A. De, S. S. Gambhir, *FASEB J* 2005, **19**, 2017–2019.
12 A. De, A. M. Loening, S. S. Gambhir, *Cancer Res* 2007, **67**, 7175–7183.

13 X. Xu, M. Soutto, Q. Xie, S. Servick, C. Subramanian, A. G Arnim, C. H. Von Johnson, *Proceedings of the National Academy of Sciences* 2007, **104**, 10264.
14 Y. Xu, D. Piston, C. A Johnson, *Proceedings of the National Academy of Sciences* 1999, **96**, 151.
15 B. Breton, E. Sauvageau, J. Zhou, H. Bonin, C. Le Gouill, M. Bouvier, *Biophysical Journal* 2010, **99**, 4037–4046.
16 A. A. Jensen, J. L. Hansen, S. P. Sheikh, H. Brauner-Osborne, *Eur J Biochem* 2002, **269**, 5076–5087.
17 D. Welsh, S. Kay, *Curr Opin Biotech* 2005, **16**, 73–78.
18 Y.-P Kim, Z. Jin, E. Kim, S. Park, Y.-H. Oh, H.-S. Kim, *Biochem Bioph Res Co* 2009, **382**, 530–534.
19 K. D. G. Pfleger, R. M. Seeber, K. A. Eidne, *Nature Protocols* 2006, **1**, 337-345.
20 K. D. G. Pfleger, R. D. Dromey, M. B. Dalrymple, E. M. L. Lim, W. T. Thomas, K. A. Eidne, *Cell. Signal* 2006, **18**, 1664-1670.
21 R. Arai, H. Nakagawa, A. Kitayama, H. Ueda, T. Nagamune, *J Biosci Bioeng* 2002, **94**, 362–364.
22 AA. Szalay, G.Wang, *U.S. Patent* US5976796, 1999.
23 A. De, P. Ray, A. M. Loening, S. S. Gambhir, *Faseb J* 2009, **23**, 2702–2709.
24 B. Branchini, J. Rosenberg, D. Ablamsky, *Analytical Biochemistry* 2011, **414**, 239–245.
25 P. Iglesias, J. A. Costoya,. *Biosens Bioelectron* 2009, **24**, 3126–3130.
26 K. Saito, N. Hatsugai, Horikawa, K.; Kobayashi, K.; Matsu-ura, T.; Mikoshiba, K.; Nagai, T. *PLoS ONE* 2010 **5**, e9935.
27 Y. Xu, A. Kanauchi, A. Arnim, von, D. Piston, C. Johnson, *Methods in enzymology* 2003, **360**, 289–301.
28 S. Gandor, S, Reisewitz, M. Venkatachalapathy, G. Arrabito, M. Reibner, H. Schroder, K. Ruf, C. M. Niemeyer, P. I. H. Bastiaens, L. Dehmelt, *Angew. Chem. Int. Ed.* 2013, **52**, 4790-4794.
29 A. Dragulescu-Andrasi, C. T. Chan, A. De, T. F. Massoud, S. S. Gambhir, *PNAS* 2011, **108**, 12060-12065.
30 N. C. Shaner, R. E. Campbell, P. A. Steinbach, B. N. G. Giepmans, A. E. Palmer, R. Y. Tsien, *Nat Biotechnol* 2004, **22**, 1567–1572.
31 A. De, P. Ray, A. M. Loening, & S. S. Gambhir, *Faseb J* 2009, **23**, 2702–2709.
32 G. H. E. Law, O. A. Gandelman, L. C. Tisi, C. R. Lowe, & J. A. H. Murray, *Biochem J* 2006, **397**, 305-312.
33 M. Bradford, *Anal Biochem* 1976, **72**, 248–254.
34 V. R. Viviani, T. L. Oehlmeyer, F. G. C. Arnoldi, & M. R. Brochetto-Braga, *Photochem Photobiol* 2007, **81**, 843–848.
35 I. Navizet, Y.J. Liu, N. Ferre, H.Y. Xiao, W.H. Fang, and R. Lindh. *J Am Chem Soc* 2009, **132**, 706–712.
36 N.Ugarova, *Photochem Photobiol Sci* (RSC Publishing). 2008.
37 T. Sandalova, & N.Ugarova, *Biochemistry* (Mosc) 1999, 926–927.
38 Rebarz, M., Kukovec, B., Maltsev, O. V., Ruckebusch, C., Hintermann, L., Naumov, P., Sliwa, M. *Chemical Science* 2013, **4**, 3803–3809.
39 D. Fink S. Wohrer M Pfeffer, T Tombe, CJ Ong, PH Sorensen, *Genesis* 2010, **48(12)**, 723-9.
40 D. Shcherbo, C. S. Murphy, G. V. Ermakova, E. A. Solovieva, T. V. Chepurnykh, A. S. Shcheglov, V. V. Verkhusha, V. Z. Pletnev, K. L. Hazelwood, P. M. Roche, S. Lukyanov, A. G. Zaraisky, M. W. Davidson, D.M. Chudakov, *Biochem J* 2009, 418, 567–574.
41 D. Shcherbo, I. I. Shemiakina, A. V. Ryabova, K. E. Luker, B. T. Schmidt, E. A. Souslova, T. V. Gorodnicheva, L. Strukova, K. M. Shidlovskiy, O. V. Britanova, A. G. Zaraisky, K. A. Lukyanov, V. B. Loschenov, G. D. Luker, D. M. Chudakov, *Nat Methods* 2010, **7**, 827–U1520.

